THE BELL SYSTEM
TECHNICAL JOURNAL

Volume 47 May–June 1968 Number 5

The Design of Active Distributed Filters

By ROBERT E. PARKIN

(Manuscript received July 13, 1967)

We develop a synthesis method which leads to simple realizations of low-pass and high-pass active filters using distributed resistance-capacitance networks. In the low-pass filter there is one distributed network terminated, through a negative impedance converter, in a load consisting of a lumped network or another distributed network. Thus we can obtain a Chebyshev-like low-pass filter which has a faster cutoff than a four pole Chebyshev realization with the same ripple. In the high-pass filter design an additional feedback element is involved. We can obtain a complex pole pair to be placed anywhere in the complex frequency plane except the real frequency axis. Design charts are given.

I. INTRODUCTION

In a recent book, P. M. Chirlian covers the main filter synthesis techniques using distributed resistance-capacitance networks.[1] This paper takes a more practical design-oriented approach. Consistent with the original terminology of Wyndrum,[2] we call the uniform distributed RC network URC. The aim here is to design active distributed filters with minimal circuit element complexity. We consider the two basic types of URC shown in Figure 1, the single URC, and the common ground high-pass double URC. The low-pass filters are synthesized with a single URC and a Linvill realization[3] and the high-pass filters by a common ground high-pass double URC and a Yanagisawa realization.[4]

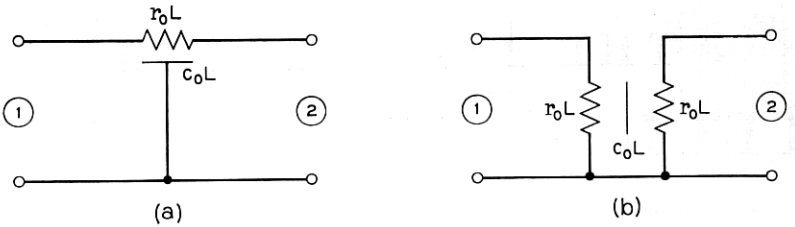

Fig. 1 — The circuit symbols for (a) the single D.C.R. and (b) the cross-connected double D.C.R.

II. THE LOW-PASS FILTER DERIVATION

2.1 *The Poles of the Transfer Function*

The transfer function for the circuit shown in Figure 2(a) can be shown to be[5]

$$\frac{V_2}{V_1} = \frac{1}{\cosh\theta - y_{NL}\dfrac{\sinh\theta}{\theta} + z_{NS}(\theta\sinh\theta - y_{NL}\cosh\theta)} \tag{1}$$

where

$$\theta = \sqrt{pr_0c_0L^2},$$

$$y_{NL} = r_0Ly_L\ ,$$

$$z_{NS} = z_S/r_0L,$$

r_0 is the resistance per unit length, c_0 is the capacitance per unit length, L is the length of the network, and p is the complex frequency variable.

If $z_S = 0$, the poles are given by

$$y_{NL} = \frac{\theta}{\tanh\theta}. \tag{2}$$

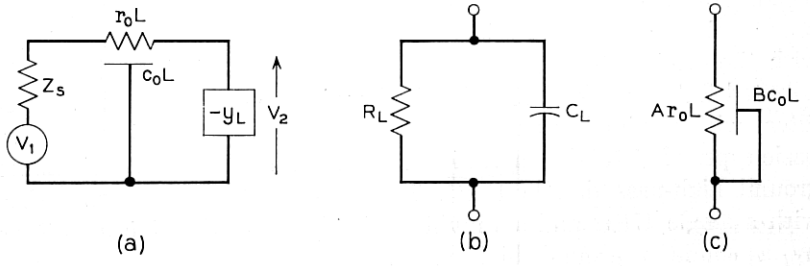

Fig. 2 — The basic low-pass filter circuit.

Notice that since $p = k\theta^2$, the negative real axis in the p plane is the imaginary axis in the θ plane.

2.2 *Lumped Load*

If the load y_L is the RC combination shown in Figure 2(b), and if $\theta = x + jy$, equation (2) becomes

$$y_{NL} \equiv \frac{1}{U} + (x + jy)^2 W = \frac{x + jy}{\tanh (x + jy)} \tag{3}$$

where

$$U = \frac{R_L}{r_0 L} \quad \text{and} \quad W = \frac{C_L}{c_0 L}.$$

An infinity of roots of equation (3) lie on the j axis of the θ plane for any U or W, and these poles are free to move[6] a maximum distance of π. When $W = 0$ (the case of resistive loading) the dominant pole pair in the θ-plane can lie at $\pm j\pi$ when $U = 0$, can move to the origin when $U = 1$, or move along the real axis towards $\pm \infty$ as $U \to 0$.

If $U = \infty$,

$$W = \frac{1}{\theta \tanh \theta} \tag{4}$$

and a pole pair caused by the capacitance loading, the loading pole pair, lies on the real axis in the θ-plane for $W > 0$. As $W \to 0$, the loading poles tend to $\pm \infty$ and in the limit $W = 0$ do not cause instability.

It is possible to choose values for U and W so that the unbounded loading and dominant poles can combine and produce roots of equation (3) for x and y nonzero. The graph of U and W for values of x and y nonzero is given in Figure 3.

The stability plot of U and W is shown in Figure 4; the plane of reference is the p plane.

Feeding the URC by a current source, the poles of V_2/I_1 can be shown to be[5]

$$y_{NL} = \theta \tanh \theta. \tag{5}$$

Again, there is a unique solution of equation (5) for x and y nonzero. For the load considered previously, the solution of equation (5) is given in Figure 5.

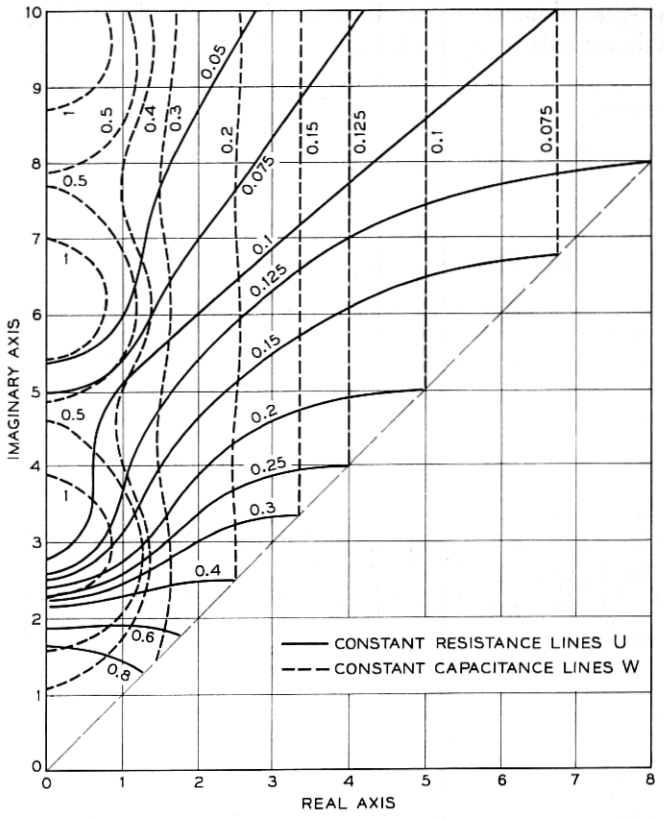

Fig. 3. — The values of U and W for complex poles at $\vartheta = x + jy$ when $z_S = 0$.

2.3 *Distributed Load*

If load y_L in Figure 2(a) is the shorted $\overline{\text{URC}}$ shown in Figure 2(c), for $z_S = 0$ the transfer function is given by

$$\frac{V_2}{V_1} = \frac{1}{\cosh\theta - \dfrac{\sqrt{B/A}\sinh\theta}{\tanh(\sqrt{AB}\cdot\theta)} + \theta\cdot z_{NS}\left[\sinh\theta - \dfrac{\sqrt{B/A}\cosh\theta}{\tanh(\sqrt{AB}\cdot\theta)}\right]} \tag{6}$$

where Ar_0 and Bc_0 are the resistance and capacitance per unit length of the load.

When $z_S = 0$, the poles are given by

$$\tanh \theta = \sqrt{A/B} \cdot \tanh (\sqrt{AB} \cdot \theta). \tag{7}$$

It is possible by suitable choice of A and B to place a pole anywhere in the θ plane. In addition, depending on the values taken by A and B, more than one complex pair of roots can occur for x and y nonzero, but no matter what values A and B assume, positioning one complex pole pair fixes all the poles of the system. When a root is positioned near the $x = y$ line in the θ plane with all other roots in the stable region, to obtain an equiripple filter, the other complex roots (if they occur) are close to the $x = 0$ line.

The solution of equation (7) for the section of the θ-plane near the $x = 6$ line is shown in Figure 6.

III. LOW-PASS FILTER DESIGN CHARTS

3.1 *Lumped Load*

From equation (1) and the load of Figure 2b, it can be seen that the position of the complex pole is determined by U, W, and z_{NS}. By choosing these three factors, the ripple in the passband is fixed. When

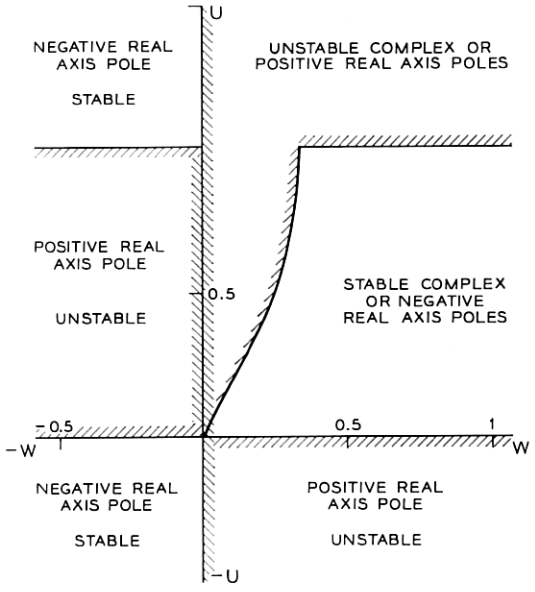

Fig. 4 — Stability plot of the low-pass lumped load filter when $z_S = 0$.

the ripple is small the complex pole pair is near the origin. When the ripple is large the complex pole pair is a long way from the origin and close to the $x = y$ line, the $j\omega$ axis in the p plane. The design chart of Figure 7 was obtained by setting $\theta = x + j(x+\delta x)$ for some value of z_{NS}, where δx is small, and determining U and W for this condition. With W held constant, U was decreased until equiripple conditions were achieved. This was repeated for a complete range of values x and z_{NS}. In addition, Figure 7 shows the conditions for constant p_c, where p_c is the 3 dB cutoff frequency.

Example

Suppose it were required to synthesize a low-pass filter with a fast cutoff having a 3 dB cutoff frequency of 75 kHz, source resistance of

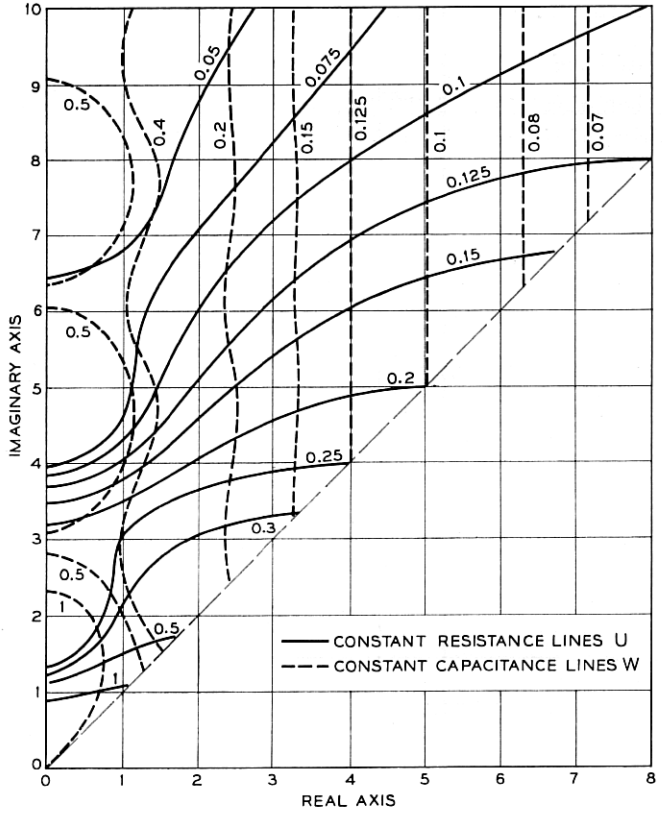

Fig. 5 — The values of U and W for complex poles at $\vartheta = x + jy$ when $z_s = \infty$.

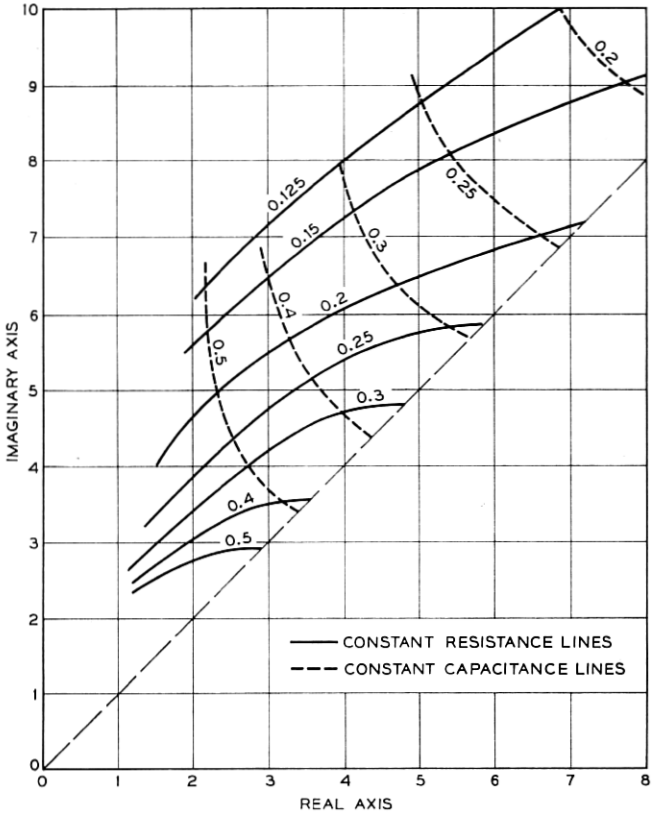

Fig. 6 — The values of A and B, the distributed load factors, for complex poles at $\vartheta = x + jy$ when $z_s = 0$.

5K Ω and working into another circuit with a driving point resistance of 10K Ω, and the maximum ripple tolerated in the passband is to be 1 dB.

If p_c is the normalized cutoff frequency,

$$r_0 L c_0 L = \frac{p_c}{7.5 \times 10^4},$$

and

$$z_{NS} = \frac{5 \times 10^3}{r_0 L}.$$

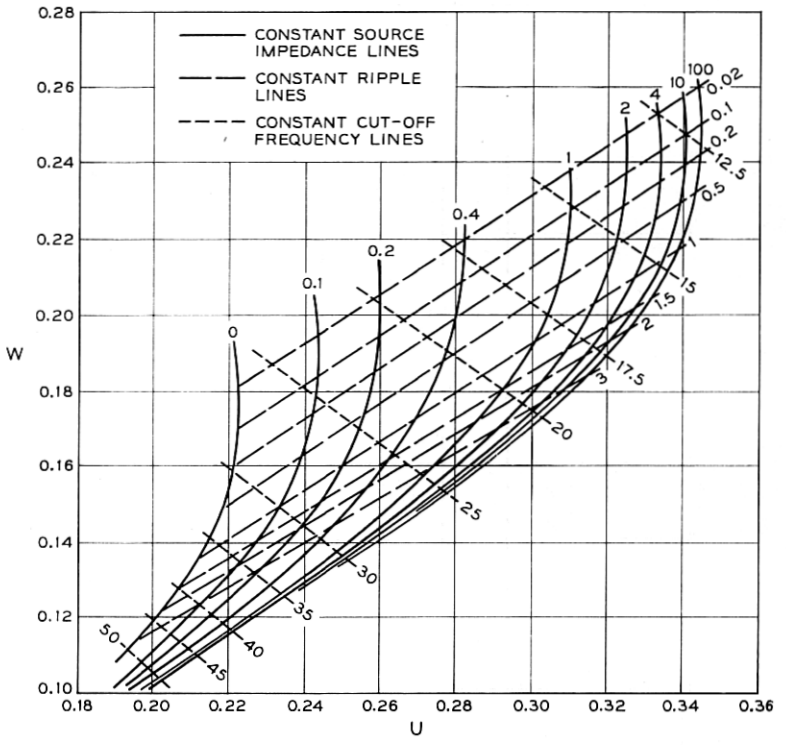

Fig. 7 — The lumped load low-pass filter design chart.

One factor can now be chosen from Figure 7, z_{NS}, r_oL, or c_oL. Letting $r_oL = 5 \times 10^4$, then

$$z_{NS} = 0.1$$

$$p_c = 30 \text{ Hz}$$

$$U = 0.2335$$

$$W = 0.150$$

Thus $c_oL = 8260$ pF. The value U is the total normalized resistor load comprising R_L and the 10K Ω driving point impedance of the next stage. The realization of the circuit is shown in Figure 8. The theoretical and measured frequency responses of this circuit are shown in Figure 9; notice the close correlation between the two. The negative impedance converter used in making the measurements is

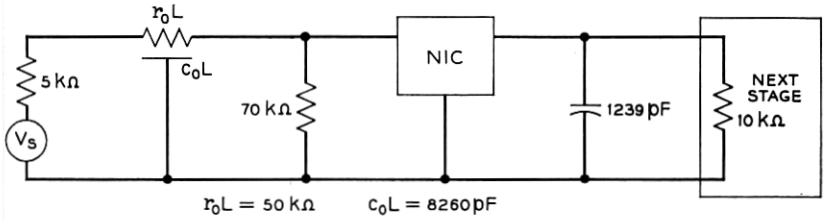

Fig. 8 — A low-pass filter circuit having lumped loading.

the NIC of Drew and Gorski-Popiel.[7] The rate of fall of the response at cutoff is 20.75 dB per octave, and the rate at the 10 dB point is 26.4 dB per octave.

3.2 *Distributed Load*

The design procedure proceeds as before, by placing the complex pole on the $x = y$ line and increasing A until equiripple conditions

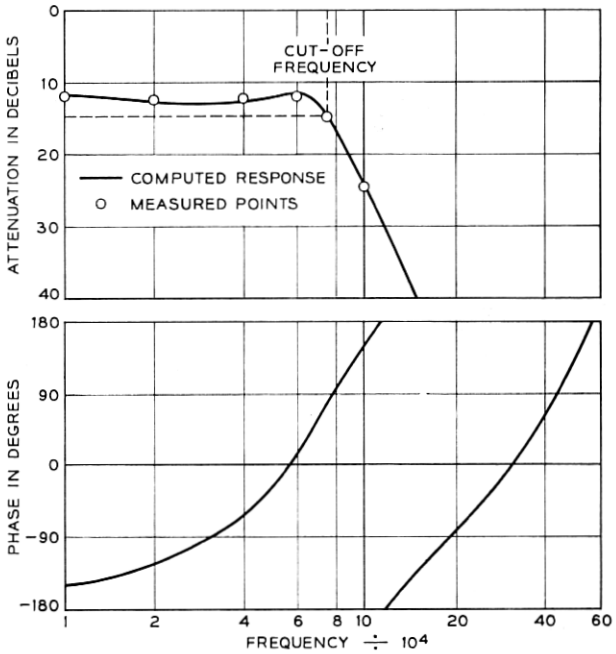

Fig. 9 — The response of the filter circuit of Fig. 8.

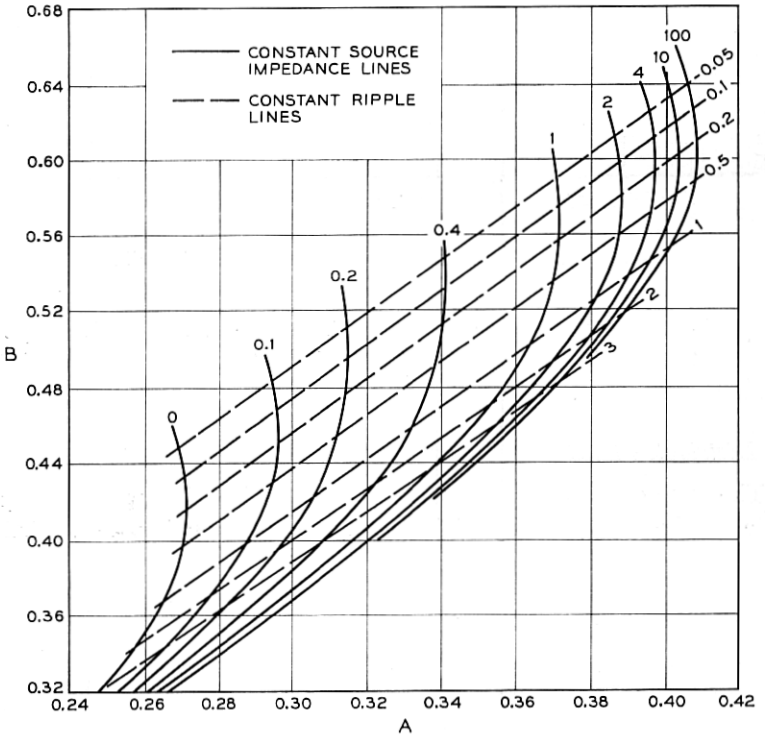

Fig. 10 — The distributed load low-pass filter design chart.

are achieved. The poles of the transfer function are given by

$$\frac{\sqrt{B/A}}{\tanh\left(\sqrt{AB}\cdot\theta\right)} = \frac{(\cosh\theta + \theta\cdot\sinh\theta\cdot z_{NS})}{(\sinh\theta + \theta\cdot\cosh\theta\cdot z_{NS})} = \alpha + j\beta. \tag{8}$$

If $(AB)^{1/2}\cdot\theta = x' + jx'$, the left side of equation (8) can be split into real and imaginary parts, so that

$$\frac{\alpha}{\beta} = -\frac{\sinh x' \cosh x'}{\sin x' \cos x'}. \tag{9}$$

Thus $(AB)^{1/2}\cdot\theta$ is calculated, and substituting in equation (8), A and B are known explicitly.

Figure 10 shows the design chart for a low-pass filter with distributed load. It was found that p_c was independent of A for any value of B, so that cutoff frequency lines were not shown in Figure 10 but were given in Figure 11.

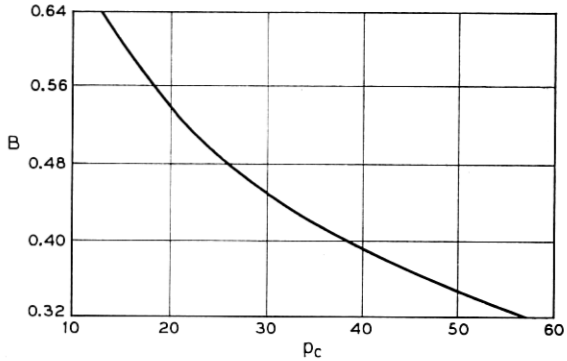

Fig. 11 — The relation between p_c and B.

Example

Using the low-pass filter with distributed load to synthesize a filter having the same requirements as in the previous example, but this time neglecting the effect of loading of the next stage, then

$$A = 0.323,$$

$$B = 0.446,$$

$$z_{NS} = 0.33,$$

$$r_0L = 1.514 \times 10^4,$$

$$c_0L = 0.0274\ \mu f,$$

for $p_c = 31$ Hz. The circuit is given for this filter in Figure 12. The measured and theoretical frequency responses are given in Figure 13. Again, notice the close correlation between the theoretical and measured frequency response. The slope of the response at cutoff is 21 dB per octave, and at the 10 dB point it is 26.75 dB per octave.

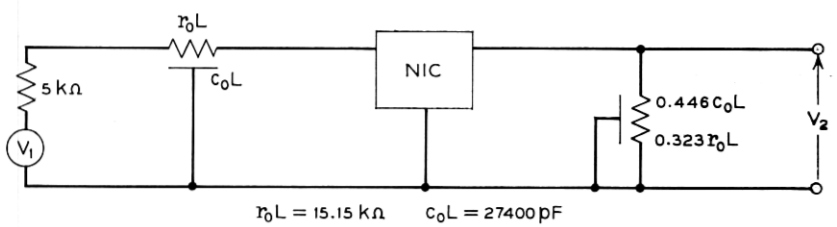

Fig. 12 — A low-pass filter circuit having distributed loading.

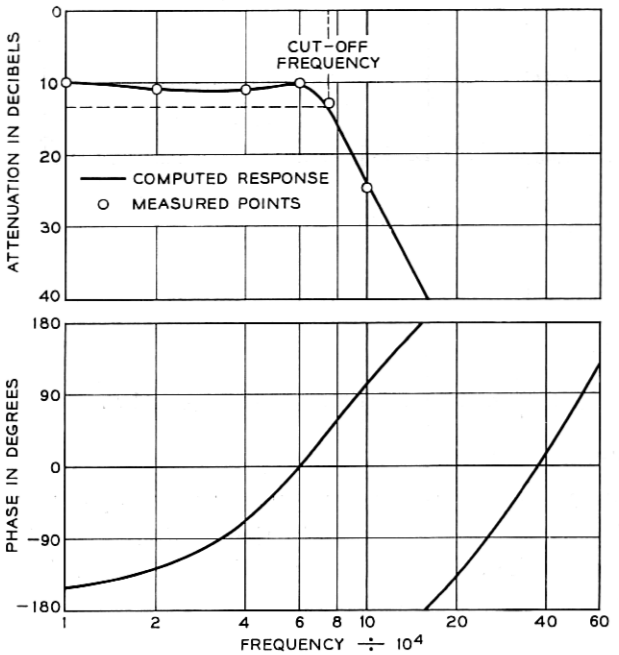

Fig. 13 — The response of the filter circuit of Fig. 12.

3.3 *Elimination of Inband Loss*

The inband loss obtained in the examples of Sections 3.1 and 3.2 can be eliminated or set to any value required by adjustment of the active device. For instance, if $-y_L$ is realized by y_L and a current inversion negative impedance converter described by

$$v_{IN} = kv_{\text{out}}$$

$$i_{IN} = ki_{\text{out}} ,$$

the equivalent form of equation (1) for $z_s = 0$ is given by

$$\frac{V_2}{V_1} = \frac{1}{k\left(\cosh\theta - \dfrac{y_{NL}\cdot\sinh\theta}{\theta}\right)}.$$

k is the factor controlling the inband loss.

IV. THE HIGH-PASS FILTER

4.1 *Transfer Function Singularities*

The parameters of the common ground high-pass $\overline{\text{URC}}$ have been developed by Hager.[8] Imbedding this element with the current negative impedance converter (current NIC) and $y_A - y_B$ networks as shown in Figure 14, the transfer function can be found as

$$\frac{V_2}{V_1} = \frac{\dfrac{\Psi}{\tanh \Psi} - 1 - 2y_{NA}}{2y_{NA} + 2y_{NB} - 1 - \dfrac{\Psi}{\tanh \Psi} + z_{NS}\left[y_{NB}\left(1 + 2y_{NA} + \dfrac{\Psi}{\tanh \Psi}\right) - \dfrac{2\Psi}{\tanh \Psi}\right]} \tag{10}$$

where

$$\Psi = \sqrt{2pr_0c_0L^2}.$$

Notice that replacement of the current NIC by a voltage NIC does not yield the same result.[5] It can be seen from Equation (10) that the loss at high frequencies is zero if and only if $z_S \to 0$ as $p \to \infty$.

When $z_S = 0$, the poles of equation (10) are given by

$$y_{NB} = \frac{1}{2} + \frac{\Psi}{2 \tanh \Psi} - y_{NA} \tag{11}$$

and the zeros by

$$y_{NA} = \frac{1}{2}\left(\frac{\Psi}{\tanh \Psi} - 1\right), \tag{12}$$

where

$$y_{NA} = r_0 L y_A \qquad \text{and} \qquad y_{NA} = r_0 L y_B .$$

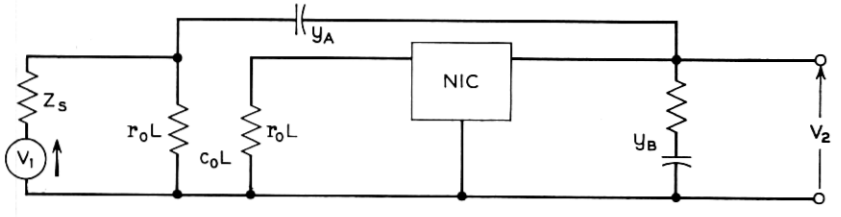

Fig. 14 — The basic high-pass filter circuit.

4.2 *Lumped Load and Feedback*

If y_A and y_B have the form shown in Figure 14, for a second order zero at the origin, equation (10) yields

$$\frac{\Psi\left(1+\frac{\Psi^2}{2!}+\cdots\right)}{\left(\Psi+\frac{\Psi^3}{3!}+\cdots\right)}-1-\Psi^2 W_F=0 \tag{13}$$

where $W_F = y_A/(pc_0L)$.

Letting $\Psi \to 0$ in equation (13), $W_F = \frac{1}{3}$ Substituting in equation (11)

$$y_{NB}\rceil = \frac{1}{2}+\frac{\Psi}{2\tanh\Psi}-\frac{\Psi^2}{3}. \tag{14}$$

There is a unique solution of equation (14) for x and y nonzero, when $x + jy = \Psi$.

4.3 *Distributed Load and Feedback*

The common ground high-pass $\overline{\text{URC}}$ is still used as the central filtering element in this high-pass filter, but the lumped elements are replaced by $\overline{\text{URCs}}$ as shown in Figure 15. Substituting for y_{NA} and y_{NB} in equation (10), and for $z_{NS} = 0$,

$$\frac{V_2}{V_2} = \frac{\dfrac{\vartheta}{\tan\vartheta}-1-\left[\dfrac{\Psi}{\dfrac{1}{\tanh\Psi}+\dfrac{\cosh\Psi-1}{\cosh\Psi+1}A}\right]}{\left[\dfrac{2(\Psi\sinh\Psi+2\cosh\Psi+2)}{A\left(\cosh\Psi+\dfrac{\sinh\Psi(\cosh\Psi+1)}{\cosh\Psi+1}\right)}-1-\dfrac{\vartheta}{\tanh\vartheta}-\dfrac{4\nu\sinh\nu}{\alpha(\nu\sinh\nu+2(\cosh\nu+1)}\right]} \tag{15}$$

where

$$\vartheta = \sqrt{2pr_0c_0L^2}$$

$$\Psi = \sqrt{2pAr_0Bc_0L^2} = \sqrt{AB}\cdot\vartheta$$

$$\nu = \sqrt{2p\alpha r_0\beta c_0L^2} = \sqrt{\alpha\beta}\cdot\vartheta.$$

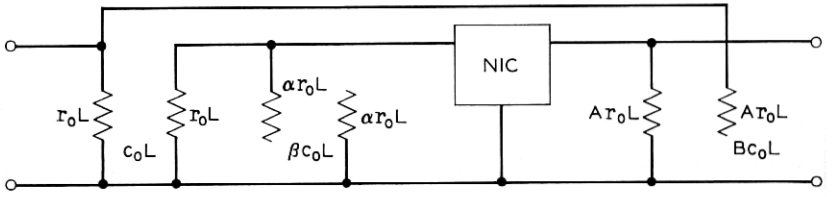

Fig. 15 — The completely distributed high-pass filter circuit.

For second order zeroes to occur at the origin, $B = 1/3$.
Notice the similarity to the previous result.

V. HIGH-PASS FILTER DESIGN

A high-pass filter can be realized from the circuit of Figure 14 by replacing y_B with a resistor R_L and capacitor C_L in series, and y_A by a capacitor. Unfortunately, to place the complex poles where required could require $R_L > 0$, $C_L < 0$. To make $C_L > 0$, connect another resistor R_1 on the other port of the NIC.

To assess the best position for the complex poles, three factors can be used which, when minimized simultaneously, produce desirable properties in the filter.

(*i*) Make the slope at cutoff as near as possible to 12 dB per octave, the low-frequency rate of change of attenuation.
(*ii*) Make the difference between the frequency at which the response crosses the constant attenuation line passing through the high-frequency attenuation, and the frequency at which a 12 dB per octave line drawn at the cut-off point would cross the high-frequency line, a minimum.
(*iii*) Make the overshoot a minimum.

These three factors are shown in Figure 16, where $G_1 = 12$, the slope of the response line at cutoff in dB per octave, $G_2 =$ the frequency at which the response attenuation is equal to the high-fre-

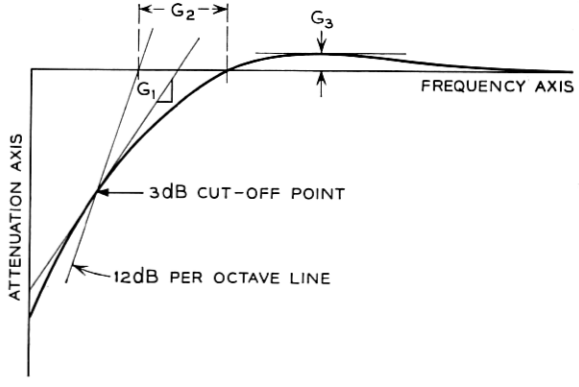

Fig. 16 — Three factors governing the quality of the high-pass filter.

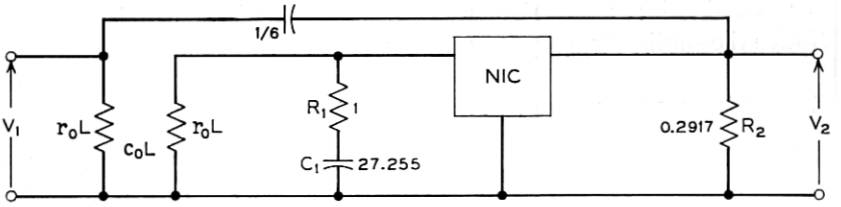

Fig. 17 — A lumped load and feedback high-pass filter.

quency attenuation $-1.25 \times$ (cutoff frequency), and G_3 = peak overshoot. Combining these three factors together as

$$G = G_1 + G_2' + G_3$$

where

$$G_2' = \frac{40G_2}{1.25 \times \text{(cutoff frequency)}}$$

and minimizing G, the best filter under these circumstances if $z_S = 0$ and the overshoot is limited to 1.25 dB, is shown in Figure 17. The response of this filter is shown in Figure 18. Notice that G_2 is slightly

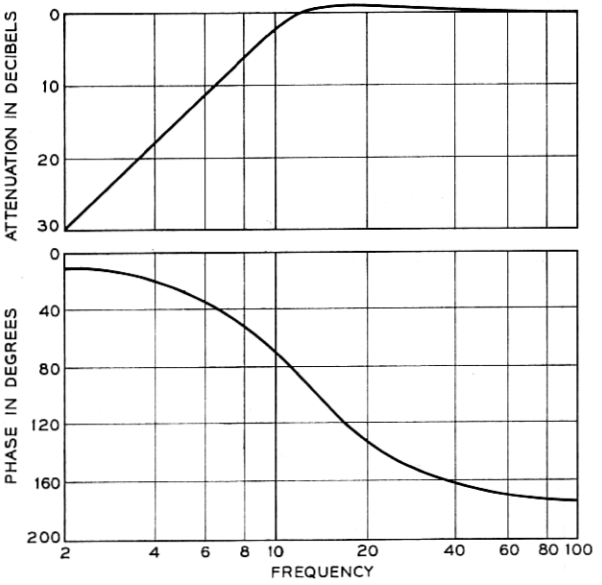

Fig. 18 — The response of the circuit of Fig. 16.

modified to G_2' to normalize for the cutoff frequency, and to introduce a loading factor.

VI. CONCLUDING REMARKS

It is evident that for best filtering characteristics, the $\overline{\text{URC}}$ must be connected to use its transmission line properties. The low pass filters use a $\overline{\text{URC}}$ as a transmission line, and the negative-valued loads serve merely to boost the high-frequency responses and extend the cutoff frequencies in a way not unlike that employed in video amplifiers, where an inductor is often used to compensate the high-frequency capacitive drop in the response.[9]

The completely distributed low-pass filter has a faster cutoff than the partially distributed filter. The difference in response is caused by the slightly different noncomplex pole positions near the origin; the further away the first negative real axis pole in the p plane is from the origin, and so closer to the other noncomplex poles, the further away the complex poles must be from the origin and nearer the limit of stability line to obtain an equiripple filter. Thus, the cutoff frequency is higher, the effect of the nondominant poles lying on the negative real axis of the p plane on the transfer function at frequencies about cutoff is more pronounced, and a faster cutoff results.

For frequencies up to the 20 dB point, to obtain an equivalent response to that of the distributed low-pass filter in lumped circuitry, would require at least five resistors and five capacitors.

To improve the response of the high-pass filters would require a higher order zero at the origin than the second order zero now obtained. Until this is achieved with a minimum of active devices, the distributed high-pass filters of the type considered here will show less promise than the low-pass filters.

Sensitivity has not been considered in this paper; to do justice to the subject would require a depth of study sufficient to warrent another paper. However, for the low-pass filters, the information contained in Figures 7 and 10 could provide a basis for future sensitivity studies.

REFERENCES

1. Chirlian, P. M., *Integrated and Active Network Analysis and Synthesis,* New York: Prentice-Hall, 1967.
2. Wyndrum, R. W. Jr., "The Exact Synthesis of Distributed RC Networks,"

N. Y. U. Technical Report 400–76, (May 1963). Abbreviated version, "The Realization of Monomorphic Thin Film Distributed RC Networks" IEEE Conv. Record, 1965, part 10, pp. 90–95.
3. Linvill, J. G., "RC Active Filters," Proc. IRE, Vol. 42, March 1954, pp. 555–564.
4. Yanagisawa, T., "RC Active Networks Using Current Inversion Type Negative Impedance Converters," IRE Trans. Circuit. Theory, *CT-4,* No. 3 Linvill (September 1957), pp. 140–144.
5. Castro, P. S. and Happ, W. W., "Distributed Parameter Circuits and Microsystems Electronics," Proc. Nat. Elec. Conf., Chicago, Ill., *16* (October 1960), pp. 448–460.
6. Parkin, R. E., "Approximations to the Equations Describing Distributed RC Networks," IEEE Trans. Circuit Theory, *CT-12,* No. 4 (December 1965), pp. 598–601.
7. Drew, A. J. and Gorski-Popiel, J., "Directly Coupled Negative Impedance Converter," Proc. IEEE, *111,* No. 7 (July 1964), pp. 1282–1283.
8. Hager, C. K., "Network Design of Microcircuits," Electronics, September 4, 1959, pp. 44–49.
9. Terman, F. E., *Electronic and Radio Engineering,* New York: McGraw-Hill, 1955, p. 292.